Journal of Medicinal Chemistry

Article

pubs.acs.org/jmc

p-(4-Azipentyl)propofol: A Potent Photoreactive General Anesthetic Derivative of Propofol

Deirdre S. Stewart,[†,⊥] Pavel Y. Savechenkov,[∥,⊥] Zuzana Dostalova,[†] David C. Chiara,[§] Rile Ge,[†] Douglas E. Raines,[†] Jonathan B. Cohen,[§] Stuart A. Forman,[†] Karol S. Bruzik,[∥] and Keith W. Miller*[,†,‡]

[†]Department of Anesthesia, Critical Care and Pain Medicine, Massachusetts General Hospital, 32 Fruit Street, Boston, Massachusetts 02114, United States

[‡]Department of Biological Chemistry and Molecular Pharmacology and [§]Department of Neurobiology, 220 Longwood Avenue, Harvard Medical School, Boston, Massachusetts 02115, United States

[∥]College of Pharmacy, University of Illinois at Chicago, 833 S. Wood Street (M/C 781), Chicago, Illinois 60612-7231, United States

ABSTRACT: We synthesized 2,6-diisopropyl-4-[3-(3-methyl-3*H*-diazirin-3-yl)propyl]phenol (*p*-(4-azipentyl)propofol), or *p*-4-AziC5-Pro, a novel photoactivable derivative of the general anesthetic propofol. *p*-4-AziC5-Pro has an anesthetic potency similar to that of propofol. Like propofol, the compound potentiates inhibitory $GABA_A$ receptor current responses and allosterically modulates binding to both agonist and benzodiazepine sites, assayed on heterologously expressed $GABA_A$ receptors. *p*-4-AziC5-Pro inhibits excitatory current responses of nACh receptors expressed in *Xenopus* oocytes and photoincorporates into native nACh receptor-enriched *Torpedo* membranes. Thus, *p*-4-AziC5-Pro is a functional general anesthetic that both modulates and photoincorporates into Cys-loop ligand-gated ion channels, making it an excellent candidate for use in identifying propofol binding sites.

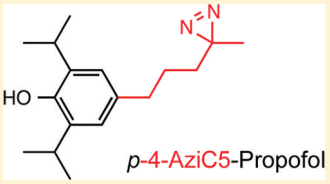

■ INTRODUCTION

Propofol is the most widely used intravenous general anesthetic for induction and maintenance of anesthesia.[1] Its advantages include both rapid-onset and rapid-recovery from anesthesia accompanied with relatively few of the common side effects of general anesthetics, such as postoperative nausea and vomiting. Many lines of evidence suggest that one of the main pharmacological actions for general anesthetics is the potentiation of the type A γ-aminobutyric acid ($GABA_A$) receptor's inhibitory response.[2−7] $GABA_A$ receptors are a member of the Cys-loop superfamily of pentameric ligand gated ion channels that also includes glycine, serotonin ($5\text{-}HT_3$), and nicotinic acetylcholine (nACh) receptors. In addition to intravenous and volatile anesthetics, $GABA_A$ receptors are modulated by a number of other classes of drugs, including neurosteroids, benzodiazepines, and ethanol.[8,9]

Identifying the binding sites of these different classes of drugs on the $GABA_A$ receptor is of major interest for understanding their mechanisms of action and for further drug development. Although mutagenesis and genetic experiments have been successful for identifying residues involved in the action of general anesthetics, the use of affinity labels is more likely to identify residues involved in a binding pocket. Experiments using a photoreactive analogue of etomidate ([^{3}H]-azietomidate) identified two residues (αMet236 and βMet286) as contributing to an intersubunit etomidate binding site, only one of which had been implicated by earlier mutagenesis experiments.[10] Both propofol and etomidate can potentiate the $GABA_A$ receptor's current response and can directly activate the receptor, activities that correlate with the drugs' in vivo anesthetic potency. The similarity in these drugs' mechanisms of action leads to the question of whether or not they act at the same site on the $GABA_A$ receptor. [^{3}H]-Azietomidate photolabeling assays on bovine brain $GABA_A$ receptors support the idea that etomidate and propofol may act through different sites.[11] Recent crystallographic studies on a bacterial homologue of the pentameric receptors from *Gloebacter violaceus* (GLIC) have identified an intrasubunit binding site for propofol and volatile anesthetics, in contrast to the intersubunit binding site identified for etomidate in the $GABA_A$ receptor.[10,12]

The development of propofol-based photoaffinity reagents is critical for identifying residues that interact with this important drug in mammalian receptors. One such reagent has been synthesized, 2-isopropyl-5-[3-(trifluoromethyl)-3*H*-diazirin-3-yl]phenol (*m*-TFD-propofol), a propofol analogue with an alkyldiazirinyl group placed at the meta-position of the phenyl ring.[13] To further investigate the nature of propofol's binding site, we have now synthesized 2,6-diisopropyl-4-[3-(3-methyl-3*H*-diazirin-3-yl)propyl]phenol (*p*-(4-azipentyl)propofol), or *p*-4-AziC5-Pro (**6**), an analogue that keeps the core propofol structure intact by adding the reactive diazirine group at the para-position of the phenol ring (Scheme 2). Here, we describe its synthesis and initial pharmacologic characterization. It functions as a general anesthetic and interacts with the $GABA_A$ and nACh receptor ligand-gated ion channels. Importantly, the *p*-4-AziC5-Pro derivative differs from the previously described photoreactive propofol (*m*-TFD-propofol) in the location of

Received: August 1, 2011
Published: October 26, 2011

dx.doi.org/10.1021/jm200943f|*J. Med. Chem.* 2011, 54, 8124−8135

Scheme 1[a]

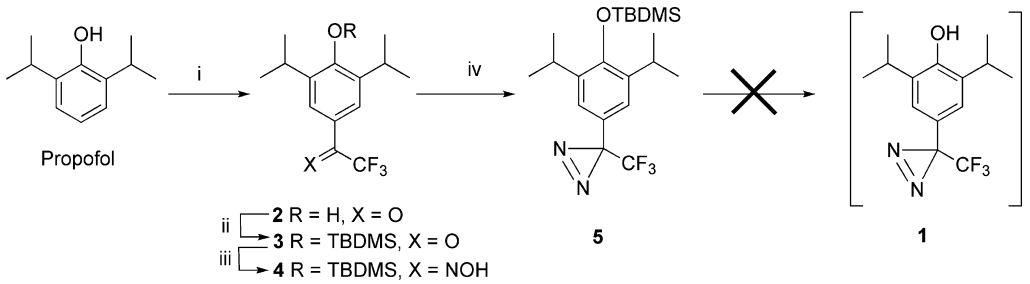

[a](i) TFAA, $AlCl_3$, DCM; (ii) TBDMSCl, imidazol, DMF; (iii) NH_2OH, HCl, Py, MeOH; (iv) (a) TsCl, Py, DCM; (b) NH_3, MeOH; (c) I_2, TEA, MeOH.

Scheme 2[a]

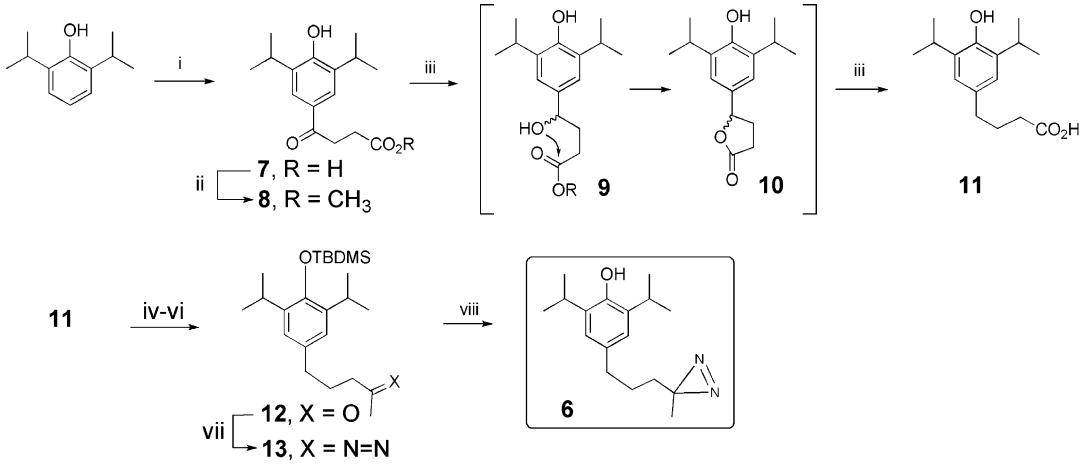

[a](i) Succinic anhydride, $AlCl_3$; (ii) MeOH, $SOCl_2$; (iii) $NaBH_4$; (iv) TEA, BOP, *N*,*O*-dimethylhydroxylamine; (v) TBDMSCl, imidazole; (vi) MeLi; (vii) (a) NH_3, MeOH, NH_2OSO_3H; (b) I_2, TEA, MeOH; (viii) CsF, EtOH.

Scheme 3[a]

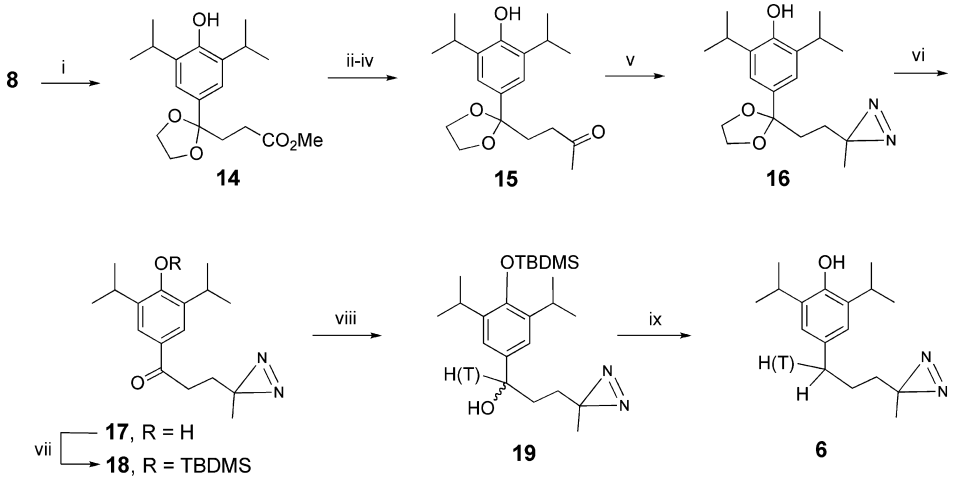

[a](i) Ethylene glycol, $(MeO)_3CH$, TsOH; (ii) KOH−H_2O; (iii) TEA, BOP, NH(Me)OMe; (iv) MeLi, THF; (v) (a) NH_3, MeOH, NH_2OSO_3H; (b) I_2, TEA; (vi) TFA−H_2O; (vii) TBDMSCl, imidazole; (viii) $NaBH_4$ or $NaBT_4$; (ix) (a) CsF; (b) Et_3SiH, TFA.

the reactive group, opening the possibility of exploring the binding site in more detail.

RESULTS

Synthesis of Diazirine Analogues of Propofol. A large number of photoaffinity reagents based on 1-aryl-1-trifluoromethyldiazirines have been described in the literature.[14] On the basis of the existing QSAR of propofol's anesthetic activity, the introduction of the trifluoromethyldiazirine moiety on the aromatic ring of propofol could be best achieved at the 4-position, since substitutions at this position do not significantly alter the anesthetic properties of propofol.[15] An alternative

dx.doi.org/10.1021/jm200943f|J. Med. Chem. 2011, 54, 8124–8135

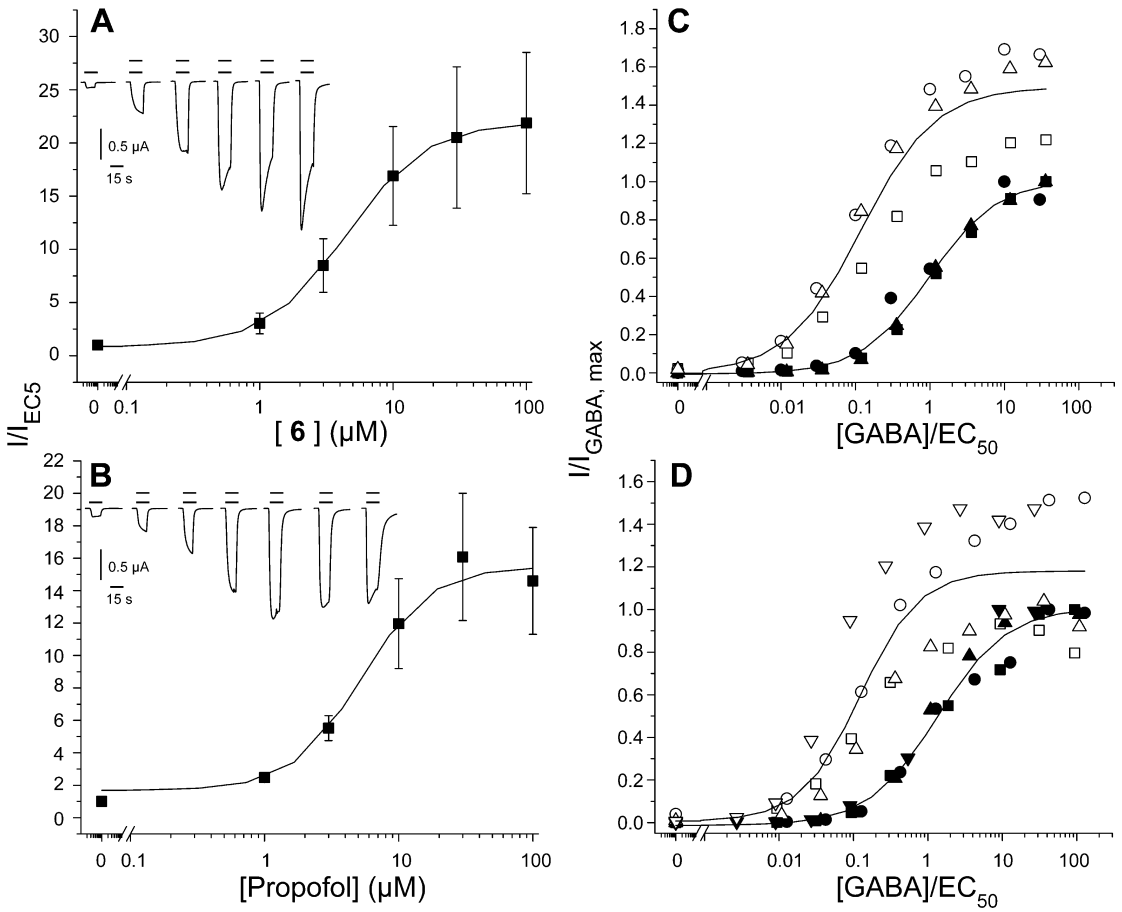

Figure 1. $GABA_A$ receptor current enhancement. (A, B) Two electrode voltage clamp was used to measure currents from oocytes injected with human $\alpha1\beta2\gamma2$L $GABA_A$ receptor subunits. Currents were elicited with 3 μM GABA ($\sim EC_5$) in the presence of increasing amounts of **6** (A) or propofol (B). Solid lines represent the nonlinear least-squares fit of the data. For **6**: EC_{50} = 4.5 ± 2.7 μM, n_H = 1.4 ± 1.3, I_{max} = 22 ± 6% (four oocytes). For propofol: EC_{50} = 5.2 ± 2.1 μM, n_H = 1.7 ± 1.2, I_{max} = 16 ± 3% (two oocytes). Insets show current traces elicited by 3 μM GABA (black bars) plus increasing amounts of drug (1, 3, 10, 30, 100 μM **6** and 1, 3, 10, 30, 100, 300 μM propofol) (gray bars). (C, D) GABA concentration–response curves shift to the left in the presence of drugs. For plotting, currents were normalized to $I_{GABA,max}$ and [GABA] was normalized to the control GABA EC_{50} for each experiment to minimize the effect of the spread of EC_{50} values of the different oocytes.[38] The data were fit as described above and in the Experimental Section for **6** (C): EC_{50} = 0.99 ± 0.11, n_H = 1.0 ± 0.1 for GABA alone (solid symbols) and EC_{50} = 0.12 ± 0.03, n_H = 0.9 ± 0.2 in the presence of 6 μM **6** (open symbols) (three oocytes). For propofol (D): EC_{50} = 1.35 ± 0.2, n_H = 0.9 ± 0.1 for GABA alone (solid symbols) and EC_{50} = 0.12 ± 0.04, n_H = 1.1 ± 0.3 in the presence of 4.4 μM propofol (open symbols) (four oocytes).

strategy involves the removal of one of the isopropyl groups and modification of the 3-position.[13]

As our first synthetic target, we selected 4-trifluoromethyldiazirynylpropofol (**1**, 4-TFD-Pf) (Scheme 1). The intermediate **5** was synthesized in a sequence of Friedel–Crafts acylation, phenol protection with dimethyl-*tert*-butylsilyl group, and assembly of the diazirine group by a routine procedure. However, the final deprotection of the diazirine **5** failed to produce a stable product. We have tried without success a variety of deprotecting conditions, including TBAF, TBAF–acetic acid, HF, pyridine–HF, TsOH, and HCl. The rapid decomposition of the target compound **1** is most likely due to the electronic effect of the hydroxy group in the para-position stabilizing the benzylic carbene. Indeed, syntheses of 4-hydroxyphenyldiazirine have been previously reported, but no detailed synthetic procedures were provided.[16] In contrast, the isomeric *m*-hydroxyphenyldiazirines are stable.[17]

To avoid this source of instability, we redesigned the photoactivatable analogue of propofol to separate the diazirine moiety from the phenyl ring. In the new analogue **6** (Scheme 2), the photoaffinity label is linked to the propofol core via a short nonpolar spacer. The synthetic expediency and the necessity to maintain a nonpolar environment at the bottom of the ring suggested a three-carbon linker.

The synthesis of the diazirine **6** shown in Scheme 2 started with an acylation of propofol with succinic anhydride to give the key intermediate **7**. The next steps involved esterification of the carboxyl group and an unusual direct reduction of the ketoester **8** into the acid **11**. Interestingly, such a reduction has not been previously reported, and the model $NaBH_4$ reduction of the keto group in 4-acetylpropofol stops at the stage of a corresponding alcohol. We hypothesize that the initially formed alcohol **9** is first converted into the lactone **10** and that the activation of the hydroxyl group by an ester enables further reduction of the C–O bond. Thus, the ketone group in **8** is converted into a methylene group in **11** via a one-step procedure and under very mild conditions. The carboxylic acid **11** was next converted into the corresponding ketone **12** using a Weinreb procedure,[18] and the subsequent diazirination by the modified method of Church and Weiss[19] followed by deprotection of the phenol afforded the target diazirine **6**.

dx.doi.org/10.1021/jm200943f|J. Med. Chem. 2011, 54, 8124–8135

For the purpose of radiolabeling of **6** with tritium, an alternative synthesis was developed (Scheme 3) in which the introduction of the label was achieved by the reduction of the ketone (e.g., step iii in Scheme 2), performed at a later stage of synthesis. Thus, the keto group in the ester **8** was protected as 1,3-dioxolane to give the ketal **14**. The subsequent one-carbon elongation of the ketone **15** and assembly of the diazirine **16** were performed analogously as described in Scheme 2. The keto group was deprotected with TFA and the phenol protected with TBDMS to form the diazirine **18**. The protection of phenol with the TBDMS group was necessary to minimize decomposition of the reducing agent ($NaBH_4$ or $NaBT_4$) by the acidic phenolic OH group during the radiolabeling reduction step. The reduction of the ketone **18** with sodium borohydride afforded the alcohol **19**, and the subsequent further reduction with triethylsilane and desilylation produced the final product **6**. The tritiation at the level of 12 Ci/mmol was achieved by substituting $NaBT_4$ for $NaBH_4$ in step viii-a.

Pharmacological Properties. *Solubility and Partition Coefficient.* The saturated aqueous solubility of **6** in 0.01 M Tris-HCl, pH 7.4, was 73 ± 4 μM (all errors herein are standard deviations unless otherwise stated). At a concentration close to saturation, the compound was stable at 4 °C in the aforementioned buffer for at least 2.5 days and eluted as a single fraction at 81.5% acetonitrile when analyzed using reverse phase HPLC. The octanol/water partition coefficient was estimated to be 15 600 ± 1200. For comparison, the saturated concentration of pure propofol in water is 1 ± 0.02 mM, and the octanol/water partition coefficient is 4300 ± 280.[20]

Anesthetic Activity. The anesthetic potency of **6** was assayed in tadpoles. The concentration dependence of loss of righting reflexes (LoRR) was examined in groups of five animals at seven concentrations between 1.0 and 20 μM (ten animals per concentration). Anesthesia was reversible, the animals recovering in fresh solution overnight. The one death was not at the highest concentration, so it was likely unrelated to the agent. Only animals that fully recovered in fresh water overnight were included in the analysis. The EC_{50} determined with 69 animals was 3.2 ± 0.55 μM and the slope was 1.7 ± 0.4. Thus, **6** is a general anesthetic with potency comparable to that of propofol, which has an EC_{50} of 2.2 ± 0.2 μM.[20]

Enhancement of $GABA_A$ Receptor Channel Function. Human $\alpha1\beta2\gamma2$L $GABA_A$ receptor currents (at EC_5) expressed in *Xenopus* oocytes were potentiated with increasing amounts of **6** (Figure 1A) with an EC_{50} of 4.5 ± 2.7 μM, compared to 5.2 ± 2.0 μM for propofol (Figure 1B). At maximal concentrations of **6** (100 μM), current responses were enhanced ~20-fold (Figure 1A), similar to ~15-fold seen with 30−100 μM propofol (Figure 1B).

GABA concentration response curves (±drugs) were determined at a fixed concentration of anesthetic equal to twice the EC_{50} for tadpole anesthesia, a concentration generally considered to represent clinical anesthesia, and were shifted to the left ~9-fold by 6 μM **6** (Figure 1C) and ~11-fold by 4.4 μM propofol (Figure 1D).

Like propofol, **6** directly activated $GABA_A$ receptor currents in the absence of GABA (data not shown). The direct activation data were also fit with the nonlinear least-squares regression to the Hill equation, and **6** produced currents of 10 ± 3% of the GABA response with an EC_{50} of 15 ± 3 μM (three oocytes), whereas propofol activated the receptor 45 ± 10% of the maximal GABA response with an of EC_{50} of 50 ± 5 μM (two oocytes).

Modulation of Ligand-Binding to $GABA_A$ Receptors. To assess allosteric action, the effects of **6** were compared to those of propofol for modulating the binding of 1.5 nM [^{3}H]-flunitrazepam (benzodiazepine site) or 3 nM [^{3}H]muscimol (agonist site) to $\alpha1\beta3\gamma2$ $GABA_A$Rs (Figure 2).

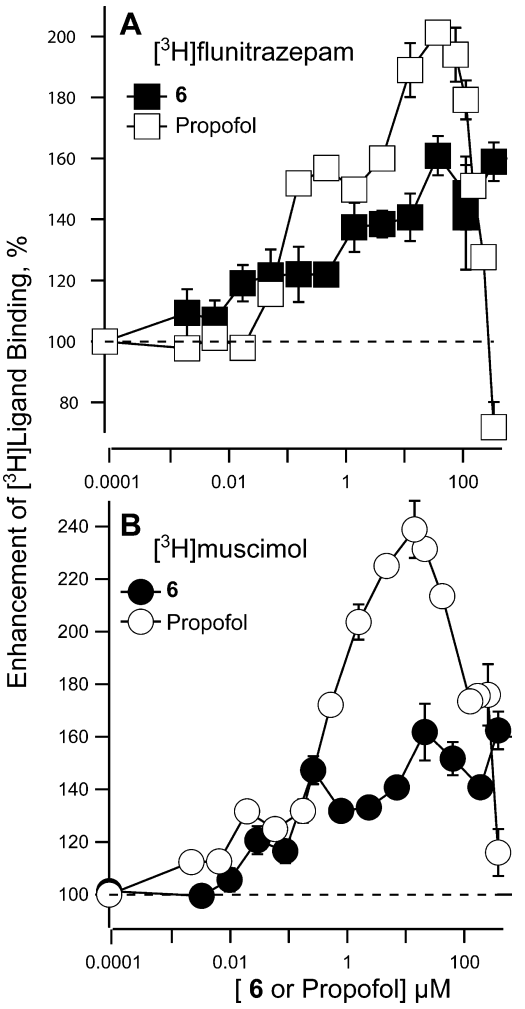

Figure 2. [^{3}H]Flunitrazepam and [^{3}H]muscimol binding to $GABA_A$ receptors. The specific [^{3}H]flunitrazepam (1.5 nM) and [^{3}H]-muscimol (3 nM) binding to membrane suspensions of $\alpha1\beta3\gamma2$ $GABA_A$ receptors heterogeneously expressed in HEK293 cells was evaluated at various concentrations of **6** or propofol. The percent enhancement of binding of three measurements are plotted as the mean ± standard deviation.

Specific binding of the benzodiazepine, [^{3}H]flunitrazepam, was enhanced by both agents between 0.1 and 40 μM (Figure 2A). Above this concentration, propofol caused a rapid decrease in binding up to 400 μM whereas **6** caused no further change. Compound **6** was less efficacious, causing a ~150% enhancement compared to ~200% for propofol. The concentration dependence and efficacy for enhancement of binding of the agonist [^{3}H]muscimol by both agents were very similar to that exhibited by [^{3}H]flunitrazepam, although propofol's efficacy was even higher than **6**'s and its effect reached a maximum at somewhat lower concentrations (Figure

dx.doi.org/10.1021/jm200943f|J. Med. Chem. 2011, 54, 8124−8135

2B). Again, propofol caused a sharp decrease in binding above 30 μM, but **6** did not.

Because the action of propofol was biphasic, we did not attempt to fit the data to a function. In the case of **6**, the enhancement is quite small when compared to the errors, but the data could be fit to a mass action curve with half effect concentrations of ~0.5 μM.

Inhibition of Torpedo nACh Receptors. In oocytes expressing *Torpedo* nACh receptors, currents elicited by 10 μM ACh (~EC_{20}) were inhibited by increasing amounts of **6** with IC_{50} = 4.0 ± 1.2 μM compared to IC_{50} = 7.3 ± 1.4 μM for propofol (Figure 3). The difference in the shapes of the current

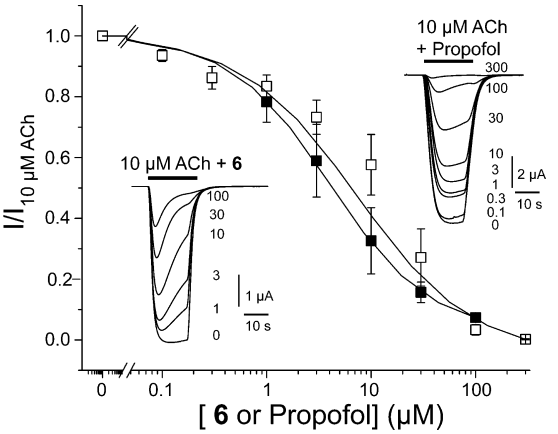

Figure 3. *Torpedo* nACh receptor current inhibition. Oocytes expressing wild type *Torpedo* nACh receptors were tested with 10 μM ACh (~EC_{20}) and then with 10 μM ACh plus increasing amounts of propofol or the propofol derivative. The current traces in the top right inset show one oocyte's current response to 10 μM ACh plus increasing amounts of propofol (0.1, 0.3, 1, 3, 10, 30, 100, 300 μM). The effect of **6** on 10 μM ACh currents is shown in the bottom left inset (1, 3, 10, 30, 100 μM). Nonlinear least-squares analysis of the curves yielded the following: for propofol (open symbols), IC_{50} = 7.3 ± 1.4 μM, n_H = 0.8 ± 0.1 (three oocytes); for **6** (solid symbols), IC_{50} = 4.0 ± 1.2, n_H = 0.9 ± 0.2 (three oocytes). Currents were normalized to the 10 μM ACh response.

traces (insets in Figure 3), with increasing amounts of compound, suggests that **6** equilibrates more slowly than propofol or possibly stabilizes the desensitized state. This hypothesis will be addressed in the future with rapid perfusion patch clamp kinetic studies.

Photoincorporation into Torpedo nACh Receptor-Enriched Membranes. Photoincorporation was assessed by SDS–PAGE followed by fluorography (Figure 4A) and liquid scintillation counting of excised gel bands (Figure 4B). For nACh receptor-rich membranes photolabeled in the absence of other drugs, there was photoincorporation in each nACh receptor subunit, with the α-subunit labeled most prominently, along with photolabeling of voltage dependent anion channel (VDAC) and the Na^+/K^+-ATPase α-subunit. In the absence of agonist, drugs that bind with high affinity with the nACh receptor ion channel either in the resting closed channel state (tetracaine) or in the desensitized state (phencyclidine) had little effect on nACh receptor subunit photolabeling. However, propofol alone increased α subunit photolabeling by ~70%. For nACh receptors desensitized in the presence of agonist (carbamylcholine), α-subunit photolabeling was increased by 100% compared to the resting state. Small additional effects on

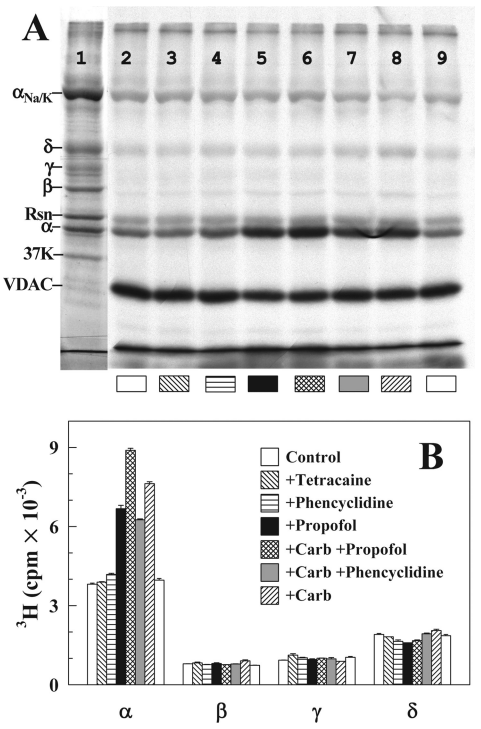

Figure 4. *Torpedo* nACh receptor photoincorporation. nACh receptor-rich membranes were photolabeled with 1.7 μM [^{3}H]**6** as described in the Experimental Section, and the polypeptides were then resolved by SDS–PAGE. (A) Polypeptides were visualized by Coomassie Blue stain (lane 1, a representative lane), and ^{3}H distribution was determined by fluorography (lanes 2–9, 14-day exposure) for aliquots photolabeled in the absence of additional drugs (lanes 2 and 9) in the presence of 100 μM tetracaine (lane 3), 100 μM phencyclidine (lanes 4 and 7), 300 μM propofol (lanes 5 and 6), and 1 mM carbamylcholine (Carb, lanes 6–8). Indicated on the left are the stained bands corresponding to the nACh receptor subunits (α, β, γ, and δ), rapsyn (Rsn), the α subunit of the Na^+/K^+-ATPase, calelectrin (37K), and the voltage dependent anion channel (VDAC).[39] (B) Quantification by liquid scintillation counting of the ^{3}H incorporation into the gel bands containing the nACh receptor subunits.

[^{3}H]**6** photoincorporation were observed when propofol (~20% increase) or phencyclidine (~20% decrease) was added to the carbamylcholine-treated samples. For the other nACh receptor subunits, the presence of agonist, propofol, or channel blockers modulated photolabeling by <20%.

DISCUSSION

Synthesis. We have synthesized **6**, a novel, photoreactive anesthetic with potency similar to that of propofol. Initial attempts to synthesize a propofol analogue with the photoreactive group at the para position, 4-TFD-propofol (Scheme 1), were unsuccessful. Therefore, we designed another strategy for obtaining a propofol derivative. To avoid the instability caused by the electronic effect of the hydroxy group in the para-position stabilizing the benzylic carbene, we redesigned the photoactivatable analogue of propofol by separating the diazirine moiety from the phenyl ring by linking to the propofol core via a short nonpolar, three-carbon spacer. The reactive aliphatic diazirine forms a carbonium ion that reacts preferentially with acidic side chains and with nucleophilic residues (tyrosine and methionine) but not with aliphatic side chains. Successful synthesis of another propofol derivative, *m*-TFD-propofol, with the photoreactive group linked directly to

dx.doi.org/10.1021/jm200943f|J. Med. Chem. 2011, 54, 8124–8135

Table 1

agent	general anesthesia $^{LoRR}EC_{50}$ (μM)	EC_{50} for EC_5 enhancement of $GABA_A$ currents (μM)	enhancement of EC_5 GABA currents at $^{LoRR}EC_{50}$	direct activation (%)	shift in GABA dose response curve	enhancement of [^{3}H] muscimol binding	enhancement of [^{3}H] flunitrazepam binding
propofol	2.2[c]	5.2[a]	4×[b]	30−50[a]	11[a]	2.4×[a]	2×[a]
	2.8[b]	1.9[d]	5×[a]	67[d]			
	1.9[d]						
6	3.2[a]	4.5[a]	8×[a]	10[a]	9[a]	1.6×[a]	1.6×[a]
m-TFD-propofol	3.1[b]	ND[e]	1.4×[b]	none[b]	ND[e]	ND[e]	ND[e]

[a]This work. [b]From Hall et al., 2010.[13] [c]From Tonner and Miller, 1995.[37] [d]From Krasowski et al., 2001.[2] [e]ND = not reported.

the benzene group at the meta position has been reported, suggesting that it is possible to synthesize a number of photoreactive propofol analogues that vary in the location, size, and type of the reactive group and yet maintain their anesthetic properties.[13] Such an array of compounds will allow for a set of tools to aid in identifying and characterizing the residues involved in propofol's binding sites.

General Anesthetic Properties. Compound **6** acts as a reversible general anesthetic in tadpoles and was approximately equipotent to the parent general anesthetic, propofol. Propofol was initially discovered during a screen of 97 alkylphenols in mice and rabbits showing that 2,6-dialkylphenols, particularly 2,6-di-*sec*-alkylphenols, were the most potent general anesthetics, while more sterically hindered analogues were inactive as anesthetics.[21] The anesthetic activity of **6** is consistent with later studies showing that substitutions at the para-position are usually well tolerated.[22,23] The potency of **6** is predicted by its octanol/water partition coefficient, in line with the empirical Meyer−Overton rule.

Effects on $GABA_A$ Receptors. The apparent affinity of GABA-elicited currents was enhanced by **6** with a potency similar to that of propofol. At twice their general anesthetic EC_{50} concentrations in tadpoles, **6** (6 μM) and propofol (4.4 μM) shifted the GABA-induced current concentration−response curve to the left by comparable amounts of 9- and 11−-fold, respectively (Figure 1C,D). This occurred without any dramatic systematic change in the maximum current elicited at high concentrations of GABA.

The concentration dependence of potentiation of currents elicited by a subsaturating EC_5 concentration of GABA for both agents was comparable. Their EC_{50} values were similar and comparable to their general anesthetic value (Table 1). The efficacy of the compounds was also similar (Figure 1A,B). The concentration dependence of potentiation is consistent with the results observed by Krasowski et al. in their study of 27 propofol derivatives where the introduction of the trifluoromethyldiazirine moiety on the aromatic ring of propofol could be best achieved at the 4-position, since substitutions at this position do not significantly alter the anesthetic properties of propofol.[2] In addition, they noted that maximum potentiation of GABA currents varied from 60% to 240%, with propofol exhibiting the greatest efficacy. In a study of 14 active propofol derivatives, two that were para-substituted had 2.5- and 4-fold lower efficacy than propofol for potentiating currents elicited by low concentrations of GABA.[2,15] In another study, out of 14 propofol derivatives substituted in the para-position, only 4 enhanced GABA currents but with efficacy similar to propofol's.[22]

In addition to enhancing GABA-induced currents, propofol alone is a very effective partial agonist, eliciting currents up to 30−70% of the maximal GABA response.[2,22] In the studies discussed above, the active para-substituted agents all directly activated with efficacies 30−100% of propofol's. Compound **6** also directly activated currents through the $GABA_A$ receptor to 10% of the maximal GABA response. In contrast, *m*-TFD-propofol at 30 μM was reported to have no direct agonist activity.[13] While halogen and aromatic 4-substitution appear to preserve efficacy for potentiation and activation,[22] the weak efficacy of the propofol photolabel derivatives adds to the small body of evidence suggesting that alkyl groups at the 3-, 4-, and 5-positions result in low efficacy.[2]

Like propofol, **6** enhanced the binding of [^{3}H]muscimol and [^{3}H]flunitrazepam to HEK293 cell membranes expressing $\alpha1\beta3\gamma2$ $GABA_A$ receptors. The subunits are arranged reading clockwise as $\alpha1\beta3\alpha1\beta3\gamma2$. Muscimol binds at the two agonist binding sites in the $\alpha-\beta$ subunit interfaces, whereas flunitrazepam binds in the $\gamma-\alpha$ subunit interface. Both sites are in the receptor's extracellular ligand-binding domain. Compound **6** potentiated both muscimol and flunitrazepam binding to similar extents, 70% and 80%, respectively, with half effect concentrations of ∼0.5 μM, well below the EC_{50} for general anesthesia. Propofol was more efficacious and had a similar concentration dependence except that at higher concentrations it caused a sharp decrease in [^{3}H]ligand binding.

Effects on nACh Receptors. The only readily available and abundant biological source for a Cys-loop receptor is the electric organ from the *Torpedo* ray, thus making the nACh receptor the most convenient member of this family for assessing a new photolabel. In this work, we photolabeled the nACh receptor in the presence of various drugs that have known sites of action and allosteric effects, thus enabling an assessment of photolabeling efficacy and specificity. The nACh receptor has five subunits ($2\alpha,1\beta,1\gamma,1\delta$) that exhibit homologous secondary structure. A large extracellular agonist-binding domain is followed by a transmembrane domain of four α-helices, M1−M4, with a large intracellular loop separating M3 and M4. The five M2 helices line the central ion-conducting pore and are the target of many drugs.

Compound **6** most efficiently photolabeled the nACh receptor α-subunit, and that photolabeling was enhanced when the receptor was in the desensitized state (Figure 4). For photolabeling at 1.7 μM [^{3}H]**6**, the 3000 cpm of carbamylcholine-enhanced [^{3}H] photoincorporation in the nACh receptor α-subunit indicates photolabeling of 0.2% of α-subunits, an efficiency of incorporation similar to that seen for [^{3}H]TDBzl-etomidate or [^{3}H]azietomidate[24] and sufficient to allow for identification of photolabeled nACh receptor amino acids.[25,26] This photolabeling pattern was similar to that seen for azioctanol[27] and azietomidate.[25] Thus, carbamylcholine, an agonist that stabilizes the desensitized state, significantly increased the photoincorporation of **6** into the nACh receptor α-subunit. Propofol also enhanced α-subunit photolabeling in

dx.doi.org/10.1021/jm200943f|J. Med. Chem. 2011, 54, 8124−8135

both the absence and presence of agonist. The propofol enhancement of α-subunit photolabeling in the absence of agonist may occur because propofol can stabilize the nACh receptor in the desensitized state. However, in the presence of agonist the receptor is already desensitized so that when propofol further enhances photoincorporation, a second distinct site for propofol may be invoked.

We also examined the effects of two known nACh receptor channel blockers on [^{3}H]**6** photolabeling: tetracaine, which binds with high affinity to the channel when the nACh receptor is in the resting, closed channel state,[28] and phencyclidine, which binds with high affinity when nACh receptors are in the desensitized state.[29,30] The **6** binding site appears distinct from that of tetracaine, which had no effect on photolabeling in the resting state. However, the partial inhibition by phencyclidine of photolabeling suggests that there may be some **6** binding within the nACh receptor ion channel in the desensitized state. Further photolabeling studies on a larger scale are required to directly identify the nACh receptor amino acids that are photolabeled.

On the nACh receptor, **6** inhibited currents with the same potency and efficacy as propofol. The current traces observed with increasing amounts of **6** suggest a role for desensitization in its inhibitory response, consistent with the photolabeling results that show increased labeling in the desensitized state.

CONCLUSIONS

Compound **6** is a novel, photoreactive derivative of the anesthetic propofol. In most respects it acts like propofol. It causes general anesthesia at a similar concentration and modulates and activates heterologously expressed $GABA_A$ receptors. This propofol derivative also functions as a photoaffinity agent, photoincorporating into nACh receptors in a pharmacologically specific fashion. Compared to a previously developed photoactivable propofol derivative *m*-TFD-propofol, **6** has a different photoselectivity for amino acid residues. The two photoactivable derivatives of propofol have similar $GABA_A$ receptor pharmacology, but they differ in detail, and a comparison may allow for a more detailed mapping of binding sites just as it has in the case of a pair of etomidate derivatives containing an aliphatic diazirine, azi-etomidate, and an aromatic diazirine, TDBzl-etomidate.[31]

EXPERIMENTAL SECTION

Materials. [^{3}H]Muscimol (3-hydroxy-5-aminomethylisoxazole, [methylene-^{3}H(N)]) (22.46 Ci/mmol) and [^{3}H]flunitrazepam (flunitrazepam, [methyl-^{3}H]) (75.7 Ci/mmol) were from Perkin-Elmer (Waltham, MA). GABA (γ-aminobutyric acid), flurazepam dihydrochloride, propofol (2,6-diisopropylphenol, 97%), and all other chemicals and reagents, as well as solvents, including anhydrous THF, were purchased from Sigma-Aldrich (St. Louis, MO) and were used as received, without further purification. cDNAs for the α1, β2, and γ2L subunits of human $GABA_A$ receptors in pCDM8 vectors were gifts from Dr. Paul J. Whiting (Merck Sharp & Dohme Research Labs, Essex, U.K.).

Analytical Chemistry. ^{1}H, ^{13}C, and ^{19}F NMR spectra were recorded on a Bruker Avance spectrometer at 400, 100, and 376 MHz, respectively, unless otherwise noted, with TMS as an internal standard. HRMS experiments were performed with Q-TOF-2TM (Micromass). TLC was performed with Merck 60 F254 silica gel plates. Purity of the final compound was assessed by HPLC analysis with a Synergy Hydro-Rp column (4 μm, 4.60 mm × 150 mm) using methanol−water with 0.05% trifluoroacetic acid; the gradient applied was 50% MeOH at the start to 100% MeOH over 18 min, then isocratic. Elution was monitored by UV at 280 nm (aromatic absorbance). The analysis indicated purity greater than 97%.

4-Trifluoroacetylpropofol (2). Aluminum chloride (4.00 g, 30.0 mmol) was suspended in dichloromethane (150 mL) and cooled to −48 °C. Trifluoroacetic anhydride (3.06 mL, 4.62 g, 22 mmol) in dichloromethane (20 mL) was added dropwise to the stirred suspension. The resulting suspension was stirred at −48 °C for 30 min, and a solution of 2,6-diisopropylphenol (3.56 g, 20.0 mmol) in dichloromethane (20 mL) was added dropwise. The reaction mixture was stirred at the same temperature for 3 h and allowed to warm to room temperature overnight. The reaction mixture was poured onto a mixture of ice and 2.0 M HCl (150 mL each) and stirred for 1 h. The layers were separated, and the organic phase was washed with H_2O (2 × 100 mL), saturated $NaHCO_3$, and brine (100 mL each), dried over $MgSO_4$, and concentrated. The residue was chromatographed on silica gel using ethyl acetate−hexanes, 1:10, as eluent to yield pure **2** as a low-melting solid (3.18 g, 58%). ^{1}H NMR (360 MHz, $CDCl_3$): δ 7.81 (s, 2H, H_{arom}), 3.26 (sept, 2H, J = 6.8 Hz, CH-*i*-Pr), 1.24 (d, 12H, J = 6.8 Hz, CH_3). ^{13}C NMR (90.6 MHz, $CDCl_3$): δ 179.2 (q, $^2J_{C\text{-}F}$ = 33.5 Hz, C=O), 158.5, 135.8, 126.7, 117.6, 117.6 (q, $^1J_{C\text{-}F}$ = 291.0 Hz), 30.0, 22.1. ^{19}F NMR (338.8 MHz, $CDCl_3$): δ −71.7 (s). HRMS (ESI) calcd for $C_{14}H_{16}F_3O_2$: [M − H] 273.1108. Found: 273.1111.

***O*-*tert*-Butyldimethylsilyl-4-trifluoroacetylpropofol (3).** The mixture of the ketone **2** (1.00 g, 3.65 mmol), *tert*-butyldimethylsilyl chloride (660 mg, 4.38 mmol), imidazole (497 mg, 7.30 mmol), and dry DMF (5 mL) was stirred for 12 h at 20 °C. This mixture was added to hexane (50 mL), washed with water (50 mL), and the aqueous layer was extracted with hexane (2 × 20 mL). The combined organic phases were washed with water (3 × 30 mL), dried over $MgSO_4$, and concentrated under vacuum. Column chromatography on silica (1−3% of ether in hexanes as eluent) afforded the protected ketone **3** as a colorless solid (1.02 g, 72%, mp 41−44 °C). ^{1}H NMR ($CDCl_3$): δ 7.84 (unresolved q, 2H, ^5J = 0.9 Hz, CH_{arom}), 3.33 (m, 2H, J = 6.9 Hz, CH-*i*-Pr), 1.22 (d, 12H, J = 6.9 Hz, CH_3-*i*-Pr), 1.06 (s, 9H, *t*-Bu), 0.27 (s, 6H, Si-CH_3). ^{13}C NMR ($CDCl_3$): δ 179.5 (q, $^2J_{C\text{-}F}$ = 34.1 Hz, C=O), 156.6, 140.3, 126.6 (unresolved q, $J_{C\text{-}F}$ = 2.1 Hz), 123.8, 117.0 (q, $^1J_{C\text{-}F}$ = 291.8 Hz), 26.8, 26.0, 23.0, 19.0, −3.2 (CH_3-Si). ^{19}F NMR ($CDCl_3$): δ −70.6 (s). HRMS (ESI) calcd for $C_{20}H_{32}F_3O_2Si$: [M + H] 389.2218. Found: 389.2129.

1-[4-(*tert*-Butyldimethylsilyloxy)-3,5-diisopropylphenyl]-2,2,2-trifluoroethanone Oxime (4). The ketone **3** (1.00 g, 2.57 mmol), hydroxylamine hydrochloride (357 mg, 5.15 mmol), and pyridine (0.31 mL, 3.9 mmol) were refluxed with stirring in methanol (4 mL) for 2 h. The resultant clear solution was partitioned between water and 10% ethyl acetate in hexanes (40 mL each). The aqueous layer was extracted with the same solvent (2 × 20 mL). The combined organic phases were washed with water (3 × 20 mL), brine (20 mL) and dried over $MgSO_4$. Evaporation and chromatography on silica (ethyl acetate−hexanes, 1:20) afforded oxime **4** as a mixture of two isomers with 1:0.74 ratio as a low-melting solid (999 mg, 96%). ^{1}H NMR ($CDCl_3$): δ 9.49 (s, 1.7H, NOH), 7.38 (s, 2H, CH_{arom}), 7.23 (s, 1.5H, CH_{arom}), 3.42 − 3.29 (m, ~3.5H, CH-*i*-Pr), 1.21 (d, 21H, J = 6.8 Hz, CH_3-*i*-Pr), 1.08 (2 s, 16H, *t*-Bu), 0.26 and 0.24 (each s, 10.5H, CH_3-Si). ^{19}F NMR ($CDCl_3$): δ −62.3 (s, 1.26F), −65.7 (s, 1.74F). HRMS (ESI) calcd for $C_{20}H_{33}F_3NO_2Si$: [M + H] 404.2227. Found: 404.2233.

3-[4-(*tert*-Butyldimethylsilyloxy)-3,5-diisopropylphenyl]-3-trifluoromethyl-3*H*-diazirine (5). The oxime **4** (100 mg, 0.248 mmol) and *p*-toluenesulphonyl chloride (95 mg, 0.50 mmol) were dissolved in dry dichloromethane (1 mL) and cooled with stirring on an ice bath, and pyridine (0.2 mL) was added dropwise. After 1 h at 0 °C the reaction mixture was warmed to room temperature and stirred for a further 24 h, diluted with ether (3 mL), washed with water (2 × 1 mL) and saturated NaH_2PO_4 (1 mL), dried over $MgSO_4$, and concentrated. The resultant colorless oil was dissolved in methanolic ammonia (7 M, Aldrich), and the resultant yellow solution was stirred at room temperature for 2 days. The reaction mixture was then concentrated under vacuum, dissolved in methanol/triethylamine mixture (10:1, 3 mL), and cooled to 0 °C with stirring. Finely dispersed iodine (63 mg, 0.248 mmol) was added in small portions

over 15 min until the mixture remained persistently brown. The excess iodine was quenched with 5% $Na_2S_2O_3$ (1 mL). The reaction mixture was diluted with water (15 mL) and extracted with DCM (3 × 5 mL). The combined organic phases were washed with water and brine (10 mL each) and dried over Na_2SO_4. Evaporation under vacuum and chromatography on silica gel (ethyl acetate–hexanes, 1:100) afforded the diazirine **5** (32 mg, 32%) as a low-melting solid. ^{1}H NMR ($CDCl_3$): δ 6.85 (s, 2H, H_{arom}), 3.30 (sept, 2H, J = 6.9 Hz, CH-*i*-Pr), 1.16 (d, 12H, J = 6.9 Hz, CH_3-*i*-Pr), 1.03 (s, 9H, *t*-Bu), 0.20 (s, 6H, Si-CH_3). ^{13}C NMR ($CDCl_3$): δ 150.6, 140.0, 122.4 (q, $^1J_{C\text{-}F}$ = 274.8 Hz), 122.1, 121.8, 28.6 (q, $^2J_{C\text{-}F}$ = 40.0 Hz), 26.7, 26.0, 23.1, 18.9, −3.3 (Si-CH_3). ^{19}F NMR ($CDCl_3$): δ −65.2 (s) HRMS (ESI) calcd for $C_{20}H_{31}F_3N_2OSi$: 400.2158. Found: 373.2178 (M^+ − N2 + H^+, $C_{20}H_{32}F_3OSi$, 373.2180).

Attempted Desilylation of Diazirine 5. In a typical experiment, TBAF (1 mL, 1 M in THF) was cooled to 0 °C and mixed with acetic acid (mixtures from 1 to 5 equiv of AcOH were used). Diazirine **5** (5.0 mg, 0.012 mmol) was dissolved in this TBAF–AcOH–THF mixture with stirring, and the reaction was monitored by TLC. After completion, the reaction mixture was poured onto crushed ice (10 mL) and extracted with ether (2 × 5 mL). After aqueous workup, TLC indicated that the initially formed compound decomposed into a complex mixture of several new products.

4-(4-Hydroxy-3,5-diisopropylphenyl)-4-oxobutyric Acid (7). Finely powdered succinic anhydride (6.73 g, 67.3 mmol) was added in small portions to a stirring suspension of $AlCl_3$ (29.9 g, 224 mmol) in dry dichloromethane (300 mL). The reaction mixture was stirred at room temperature for 30 min, cooled to −78 °C, and the solution of 2,6-diisopropylphenol (10 g, 56 mmol) in dichloromethane (40 mL) was added dropwise over 30 min. The resultant yellowish suspension was allowed to warm up overnight. The progress of the reaction was monitored with ^{1}H NMR. The reaction mixture was cooled to −10 °C, poured onto crushed ice (500 g), and warmed to room temperature with stirring (1 h). Organic and aqueous phases were separated, the aqueous layer was extracted with dichloromethane (4 × 100 mL), the combined organic phases were washed with brine (200 mL) and dried over $MgSO_4$. Concentration followed by drying under vacuum gave a dark-brown oil which was added to a solution of KOH (12 g, 214 mmol) in methanol/water, 1:1 (100 mL), and stirred for 2 h. The resultant solution was diluted with water (0.5 L), acidified to pH 10 with HCl, and washed with ether (3 × 100 mL). The aqueous layer was acidified to pH 3 and extracted with dichloromethane (5 × 100 mL). The combined extracts were washed with water and brine (100 mL each), dried over $MgSO_4$, and concentrated. Crystallization from ethyl acetate–hexane, 1:9, gave the acid **7** as off-white crystals (3.00 g, 19%), mp 146–147.5 °C. ^{1}H NMR ($CDCl_3$): δ 12 − 9 (br s, 1H, COOH), 7.77 (s, 2H, CH_{arom}), 5.6–5.3 (br s, 1H, ArOH), 3.33 (t, 2H, J = 6.6 Hz, CH_2), 3.18 (sept, 2H, J = 6.9 Hz, CH-*i*-Pr), 2.82 (t, 2H, J = 6.6 Hz, CH_2), 1.31 (d, 12H, J = 6.9 Hz, CH_3). ^{13}C NMR ($CDCl_3$): δ 197.1 (C═O), 178.7 (COOH), 154.8, 133.7, 129.3, 124.4 (CH_{arom}), 32.8 (CH_2), 28.3 (CH_2), 27.2 (CH-*i*-Pr), 22.5 (CH_3-*i*-Pr). HRMS (ESI) calcd for $C_{16}H_{27}O_3$: [M + H] 279.1591. Found: 279.1594.

Methyl 4-(4-Hydroxy-3,5-diisopropylphenyl)-4-oxobutanoate (8). Methanol (40 mL) was cooled to −60 °C, and thionyl chloride (2.4 mL, 33 mmol) was added dropwise over 5 min. The resultant solution was slowly warmed to 0 °C, and the ketoacid **7** (3.00 g, 10.8 mmol) was added at once. The reaction mixture was left stirring overnight at room temperature. The resulting clear solution was diluted with dichloromethane (100 mL), cooled to −5 °C, and stirred with cold water (100 mL) for 5 min. The layers were separated. The aqueous phase was extracted with dichloromethane (2 × 30 mL), the combined organic phases were washed with water (2 × 50 mL), brine (50 mL), dried over $MgSO_4$ and concentrated. Column chromatography on silica gel (ethyl acetate–hexanes, 1:10 to 1:5) afforded the ketoester **8** as colorless crystals. Yield 2.84 g (90%), mp 74 − 76 °C. ^{1}H NMR ($CDCl_3$): δ 7.77 (s, 2H, CH_{arom}), 5.82 (s, 1H, ArOH), 3.73 (s, 3H, OCH_3), 3.33 (t, 2H, J = 6.7 Hz, CH_2), 3.19 (sept, 2H, J = 6.9 Hz, CH-*i*-Pr), 2.78 (t, 2H, J = 6.6 Hz, CH_2), 1.29 (d, 12H, J = 6.9 Hz, CH_3). ^{13}C NMR ($CDCl_3$): δ 197.3 (C═O), 173.8 (COOMe), 155.0, 133.8, 129.3, 124.3 (CH_{arom}), 51.8 (OCH_3), 33.0 (CH_2), 28.2 (CH_2), 27.1 (CH-*i*-Pr), 22.6 (CH_3-*i*-Pr). HRMS (ESI) calcd for $C_{17}H_{23}O_4$: [M − H] 291.1602. Found: 291.1616.

4-(4-Hydroxy-3,5-diisopropylphenyl)butyric Acid (11). Into a stirring solution of the ketoester **8** (1.00 g, 3.4 mmol) in ethanol (40 mL) was added an excess of sodium borohydride in several portions (total 1.287 g, 34 mmol) over 1 h. The reaction was quenched with acetone (10 mL) and water (200 mL). The reaction mixture was washed with dichloromethane (3 × 30 mL), acidified with HCl to pH 4, and extracted with dichloromethane (5 × 30 mL). The acidic extract was washed with water and brine (50 mL each) and dried over $MgSO_4$. Crystallization from hexane afforded acid **11** as colorless crystals (638 mg, 71%), mp 95–96 °C. ^{1}H NMR ($CDCl_3$): δ 11.5–9.0 (br s, 1H, CO_2H), 6.87 (s, 2H, CH_{arom}), 5.0–4.4 (br s, 1H, ArOH), 3.16 (sept, 2H, J = 6.9 Hz, CH-*i*-Pr), 2.62 (t, 2H, J = 7.5 Hz, CH_2), 2.41 (t, 2H, J = 7.5 Hz, CH_2), 1.96 (quint, 2H, J = 7.5 Hz, CH_2), 1.28 (d, 12H, J = 6.9 Hz, CH_3-*i*-Pr). ^{13}C NMR ($CDCl_3$): δ 180.2 (C═O), 148.2, 133.8, 133.1, 123.4 (CH_{arom}), 34.9 (CH_2), 33.6 (CH_2), 27.2 (CH-*i*-Pr), 26.7 (CH_2), 22.8 (CH_3-*i*-Pr). HRMS (ESI) calcd for $C_{16}H_{23}O_3$: [M − H] (263.1653). Found: 263.1662.

5-[4-(*tert*-Butyldimethylsilyloxy)-3,5-diisopropylphenyl]-pentan-2-one (12). A mixture of acid **11** (300 mg, 1.135 mmol), *N*,*O*-dimethylhydroxylamine hydrochloride (221 mg, 2.27 mmol), and (benzotriazol-1-yloxy)tris(dimethylamino)phosphonium hexafluorophosphate (753 mg, 1.7 mmol) was stirred in dry dichloromethane (3 mL) under argon for 5 min at room temperature and cooled on an ice bath. Triethylamine (0.47 mL, 3.4 mmol) was added dropwise. The reaction mixture was left at room temperature overnight, diluted with diethyl ether (20 mL), washed with water (2 × 15 mL), 0.5 M HCl, 10% Na_2CO_3, and brine (10 mL each), and dried over $MgSO_4$. Concentration under vacuum afforded crude Weinreb amide as a reddish solid. The above was added to a solution of *tert*-butyldimethylsilyl chloride (257 mg, 1.7 mmol) and imidazole (155 mg, 2.27 mmol) in dry DMF (0.5 mL) and stirred for 24 h. The resulting emulsion was partitioned between ether and water (15 mL each). The organic layer was washed with water, 0.1 M HCl, saturated $NaHCO_3$, and brine (10 mL each) and dried over $MgSO_4$. The solution was filtered, concentrated and the residue dried under vacuum. This product was dissolved in dry THF (3 mL) under argon, cooled with a dry ice–acetone bath, and a solution of methyllithium (2.1 mL, 1.6 M in ether, 3 equiv) was added dropwise. After being stirred at −78 °C for 2 h the reaction mixture was quenched with a mixture of methanol and ethyl acetate (0.5 mL each) in THF (2 mL), followed by saturated aqueous NH_4Cl (10 mL). The reaction mixture was then warmed to room temperature, extracted with ether (2 × 10 mL), and the combined organic phase was washed with water (2 × 10 mL), brine (10 mL) and dried over $MgSO_4$. Concentration followed by chromatography on silica gel (ethyl acetate–hexanes, 1:50) afforded pure **12** as a colorless oil (337 mg, 79%). ^{1}H NMR ($CDCl_3$): δ 6.84 (s, 2H, H_{arom}), 3.29 (sept, 2H, J = 6.9 Hz, CH-*i*-Pr), 2.56 (t, 2H, J = 7.5 Hz, CH_2), 2.47 (t, 2H, J = 7.5 Hz, CH_2), 2.14 (s, 3H, CH_3-C═O), 1.90 (quint, 2H, J = 7.5 Hz, CH_2), 1.17 (d, 12H, J = 6.9 Hz, CH_3-*i*-Pr), 1.04 (s, 9H, *tert*-butyl), 0.20 (s, 6H, Si-CH_3). ^{13}C NMR ($CDCl_3$): δ 209.2 (C═O), 147.2, 138.8, 134.3, 123.3 (CH_{arom}), 53.4, 43.2, 34.9, 30.0, 26.5, 26.1, 25.6, 23.5, 18.9, −3.3 (CH_3-Si). HRMS (ESI) calcd for $C_{23}H_{41}O_2Si$ [M + H] 377.2870. Found: 377.2861.

3-{3-[4-(*tert*-Butyldimethylsilyl)-3,5-diisopropylphenyl]-propyl}-3-methyl-3*H*-diazirine (13). The ketone **12** (50 mg, 0.133 mmol) was dissolved in a mixture of methanol–ether (1:1, 0.5 mL) and cooled to −40 °C. A solution of ammonia in methanol (1 mL, ∼7 M) was added dropwise with stirring. The reaction mixture was warmed to −30 °C and stirred at this temperature for 6 h. The solution of hydroxylamine-*O*-sulfonic acid (23 mg, 0.20 mmol) in methanol (0.4 mL) was added dropwise, and the resulting clear solution was left at −20 °C for 5 days with occasional stirring (the reaction progress was monitored by TLC). After completion, the reaction mixture was evaporated in vacuo, dissolved in a mixture of methanol (2 mL) and triethylamine (0.06 mL, 0.4 mmol), and cooled to −10 °C. A solution of iodine (34 mg, 0.133 mmol) in

dx.doi.org/10.1021/jm200943f|J. Med. Chem. 2011, 54, 8124–8135

dichloromethane (1 mL) was added dropwise until the mixture remained persistently light-brown in color. The excess iodine was quenched with 5% solution of $Na_2S_2O_3$ (0.5 mL). The mixture was diluted with water (15 mL) and extracted with ether (3 × 10 mL). The combined organic phases were washed with water and brine (10 mL each) and dried over Na_2SO_4. Concentration and chromatography on silica gel using 1−2% ethyl acetate in hexanes as an eluent afforded pure diazirine **13** as a colorless oil (30 mg, 58%). ^{1}H NMR ($CDCl_3$): δ 6.83 (s, 2H, H_{arom}), 3.30 (sept, 2H, J = 6.9 Hz CH-*i*-Pr), 2.53 (t, 2H, J = 7.4 Hz, CH_2), 1.58−1.44 (m, 2H, CH_2), 1.44−1.37 (m, 2H, CH_2), 1.18 (d, 12H, J = 6.9 Hz, CH_3-*i*-Pr), 1.05 (s, 9H, *t*-Bu), 1.04 (s, 3H, α-*azi*-CH_3) 0.21 (s, 6H, Si-CH_3). ^{13}C NMR ($CDCl_3$): δ 147.2, 138.8, 134.5, 123.1 (CH_{arom}), 35.1 (CH_2), 34.0 (CH_2), 26.5, 26.1, 26.0 (CH_2), 25.8 (CN_2), 23.4, 19.9 (α-*azi*-CH_3), 18.9 (Si-CMe_3), −3.3 (Si-CH_3). HRMS (ESI) calcd for $C_{23}H_{41}N_2OSi$: [M + H] 389.2983. Found: 389.2993.

2,6-Diisopropyl-4-[3-(3-methyl-3*H*-diazirin-3-yl)propyl]-phenol (6). *Method A (Scheme 2).* Diazirine **13** from the previous step (30 mg, 0.077 mmol) was deprotected with cesium fluoride (101 mg, 0.67 mmol) in ethanol or TBAF−acetic acid (1:2 molar ratio, 1 M TBAF in THF + neat acetic acid, 1 mL, overnight) to obtain crude **6**. Column chromatography on silica (ethyl acetate−hexanes, 1:20) afforded pure diazirine **6** as a colorless oil (19 mg, 52% from ketone **12**). ^{1}H NMR ($CDCl_3$): δ 6.85 (s, 2H, H_{arom}), 4.66 (br s, 1H, ArOH), 3.16 (sept, 2H, J = 6.9 Hz, CH-*i*-Pr), 2.53 (t, 2H, J = 7.5 Hz, CH_2), 1.55−1.45 (m, 2H, CH), 1.45−1.37 (m, 2H, CH_2), 1.29 (d, 12H, J = 6.9 Hz, CH_3-*i*-Pr), 1.04 (s, 3H, α-*azi*-CH_3). ^{13}C NMR ($CDCl_3$): δ 148.1, 133.6, 133.5, 123.3 (CH_{arom}), 35.1 (CH_2), 33.9 (CH_2), 27.2 (CH-*i*-Pr), 26.2 (α-*azi*-CH_2), 25.8 (CN_2), 22.8 (CH_3-*i*-Pr), 19.9 (α-*azi*-CH_3). HRMS (ESI) calcd for $C_{17}H_{25}N_2O$: [M − H] 273.1972. Found: 273.1976.

Method B. Compound **6** was also synthesized by another route permitting introduction of tritium label by a reduction of the carbonyl group in ketone **18** (Scheme 3). The solution of the ketone **18** (100 mg, 0.248 mmol) in absolute ethanol (1 mL) was stirred with sodium borohydride (47 mg, 1.24 mmol) for 1 h at room temperature. After completion of the reaction (TLC), cesium fluoride (188 mg, 1.24 mmol) was added and stirring continued for another 24 h (TLC). Then the reaction mixture was divided between hexane−ethyl acetate (5:1) and water phases (10 mL each). The aqueous phase was additionally extracted with the same solvent (2 × 5 mL), and the combined organic phases were washed with brine and dried over $MgSO_4$. The resulting solution was filtered, concentrated in vacuo, and dissolved in a mixture of dichloromethane (3 mL) and triethylsilane (0.5 mL). The reaction mixture was cooled to −30 °C. The solution of trifluoroacetic acid (0.4 mL) in dichloromethane (0.6 mL) was added dropwise, and the mixture was warmed to room temperature (0.5 h). After the usual aqueous workup, chromatography on silica gel (ethyl acetate−hexanes, 1:20) afforded the target compound **10** (61 mg, 90%) as a colorless oil, identical with that obtained via Scheme 2.

^{3}H-2,6-Diisopropyl-4-[3-(3-methyl-3*H*-diazirin-3-yl)propyl]-phenol. The tritium labeled **6** with specific radioactivity of 12 Ci/mmol was synthesized as described above by ViTrax, Placentia, CA. This compound was stored at −20 °C as a solution in ethanol containing 1 mCi/mL.

Methyl 3-(2-(4-Hydroxy-3,5-diisopropylphenyl)-1,3-dioxolan-2-yl)propanoate (14). The solution of the ketoester **8** (2.00 g, 6.84 mmol), ethylene glycol (5 mL), trimethyl orthoformate (2 mL), and *p*-toluenesulfonic acid monohydrate (66 mg, 0.34 mmol) in dichloromethane (5 mL) was stirred at room temperature for 48 h (the reaction was monitored by ^{1}H NMR). The reaction was quenched with triethylamine (1 mL), and the resulting solution was partitioned between ether and water (40 mL each). The organic phase was washed with water, brine (20 mL each), dried over $MgSO_4$, evaporated, and chromatographed on silica (ethyl acetate−hexanes, 1:10, 1% triethylamine) to afford dioxolane **14** as a viscous colorless oil that crystallized upon storage in a refrigerator (1.43, 62%, mp 84−86 °C). ^{1}H NMR ($CDCl_3$): δ 7.14 (s, 2H, H_{arom}), 4.88 (br s, 1H, ArOH), 4.06−3.96 (m, 2H, OCH_2), 3.86−3.76 (m, 2H, OCH_2), 3.67 (s, 3H, OCH_3), 3.16 (sept, 2H, J = 6.9 Hz), 2.50−2.42 (m, 2H, CH_2), 2.28−2.20 (m, 2H, CH), 1.29 (d, 12H, J = 6.9, Me_2CH). ^{13}C NMR ($CDCl_3$): δ 174.1 (C═O), 149.7, 133.8, 133.3, 120.8 (CH_{arom}), 109.8 (O-C-O), 64.6 (OCH_2), 51.5 (OCH_3), 35.6 (CH_2), 28.7 (CH_2), 27.3 (CH-*i*-Pr), 22.7 (CH_3-*i*-Pr). HRMS (ESI) calcd for $C_{19}H_{29}O_5$: [M + H] 337.2010. Found: 337.2014.

4-(2-(4-Hydroxy-3,5-diisopropylphenyl)-1,3-dioxolan-2-yl)-butan-2-one (15). Ester **14** (1.80 g, 5.35 mmol) was dissolved in methanol (20 mL), and a solution of KOH (2.0 g, 36 mmol) in water (10 mL) was added at once. The reaction mixture was stirred at room temperature for 2 h (the progress was monitored by TLC), poured into 100 mL of water, and carefully acidified with 10% H_3PO_4 to pH 3. The resulting emulsion was extracted with dichloromethane (5 × 20 mL). The extracts were combined and added with triethylamine (3 mL), dried over $MgSO_4$, evaporated, and dried at 0.1 mmHg and 100 °C for 1 h. The residual solid was cooled to 0 °C (with stirring under argon) and mixed with a dichloromethane solution (20 mL) of triethylamine (2.24 mL, 3 equiv), *N*,*O*-dimethylhydroxylamine hydrochloride (0.783 g, 8.03 mmol), and (benzotriazol-1-yloxy)tris-(dimethylamino)phosphonium hexafluorophosphate (3.55 g, 8.03 mmol). The resulting dark-red suspension was stirred overnight. After the completion of the reaction (monitored by TLC, ether−hexane, 1:1, with small amount of 7 M ammonia in methanol), the reaction mixture was stirred with water (20 mL) and diluted with dichloromethane (100 mL). The layers were separated. The organic layer was washed with brine (50 mL), dried over $MgSO_4$, evaporated, and filtered through a short silica gel column (eluted with ethyl acetate/hexanes, 1:3, 1% triethylamine). The concentration of eluate afforded a dark-red oil (2.5 g). This product was dissolved in anhydrous THF (40 mL), cooled to −78 °C with vigorous stirring, and a solution of methyllithium (10 mL, 1.6 M in ether, 3 equiv) was added dropwise. The solidified reaction mixture was warmed to −20 °C for 5 min, cooled to −78 °C, and quenched with ethyl acetate (10 mL), ethyl acetate−acetic acid, 1:1 (5 mL), and water (50 mL). The usual workup (as above), followed by chromatography on silica gel (ethyl acetate−hexanes, 1:10, 1% triethylamine) afforded ketoketal **15** as a viscous colorless oil (1.07 g, 62%) (crystallized upon storage at 4 °C, mp 67−72 °C). ^{1}H NMR ($CDCl_3$): δ 7.12 (s, 2H, H_{arom}), 5.11 (br s, 1H, ArOH), 4.05−3.95 (m, 2H, OCH_2), 3.85−3.75 (m, 2H, OCH_2), 3.18 (sept, 2H, J = 6.9 Hz, CH-*i*-Pr), 2.55 (t, 2H, J = 7.5 Hz, CH_2), 2.20 (t, 2H, J = 7.5 Hz, CH_2), 2.14 (s, 3H, CH_3C═O) 1.27 (d, 12H, J = 6.9, CH_3-*i*-Pr). ^{13}C NMR ($CDCl_3$): δ 208.8 (C═O), 149.8, 133.8, 133.5, 120.7 (CH_{arom}), 110.0 (O-C-O), 64.5 (OCH_2), 38.2 (CH_2), 34.7 (CH_2), 29.8, 27.2, 22.8 (CH_3-*i*-Pr). HRMS (ESI) calcd for $C_{19}H_{29}O_4$: [M + H] 321.2060. Found: 321.2067.

2,6-Diisopropyl-4-(2-(2-(3-methyl-3*H*-diazirin-3-yl)ethyl)-1,3-dioxolan-2-yl)phenol (16). Diaziridination of ketoketal **15** was accomplished by a procedure similar to that used in the synthesis of **13** (Scheme 2). The crude product was purified by silica gel chromatography using ethyl acetate−hexanes, 1:10, with 1% of triethylamine as eluent. Starting from 1.00 g of **15**, 330 mg of diazirine **16** (32%) was obtained as a colorless oil that slowly crystallized upon storage at 4 °C, mp 30−35 °C. ^{1}H NMR ($CDCl_3$): δ 7.10 (s, 2H, CH_{arom}), 4.85 (br s, 1H, ArOH), 4.03−3.93 (m, 2H, OCH_2), 3.83−3.73 (m, 2H, OCH_2), 3.16 (sept, 2H, J = 6.9 Hz), 1.84−1.76 (m, 2H, CH_2), 1.48−1.40 (m, 2H, CH_2), 1.29 (d, 12H, J = 6.9, CH-*i*-Pr), 0.99 (s, 3H, α-*azi*-CH_3). ^{13}C NMR ($CDCl_3$): δ 149.7, 133.9, 133.3, 120.7 (CH_{arom}), 109.9 (O-C-O), 64.5 (OCH_2), 34.9 (CH_2), 28.8 (CH_2), 27.3 (CH-*i*-Pr), 25.7 (CN_2), 22.7 (CH_3-*i*-Pr), 19.7 (α-*azi*-CH_3). HRMS (ESI) calcd for $C_{19}H_{28}N_2O_3$: [M + H] 333.2173. Found: 333.2178.

1-(4-Hydroxy-3,5-diisopropylphenyl)-3-(3-methyl-3*H*-diazirin-3-yl)propan-1-one (17). Diazirine **16** (200 mg, 0.6 mmol) was dissolved in dichloromethane (3 mL), cooled to −20 °C, and trifluoroacetic acid (0.5 mL) was added dropwise with stirring. The reaction mixture was allowed to warm to 0 °C, and water (1 mL) was added. Stirring continued for 3 h (TLC was used to monitor the reaction). Water (5 mL) was added, and the layers were separated. The aqueous phase was extracted with dichloromethane (2 mL), and the combined organic phases were washed with water and brine (5 mL each; *the product is unstable under basic conditions*) and dried over

$MgSO_4$. Evaporation of solvent under vacuum left pure **17** as white crystals (163 mg, 94%), mp 87−90 °C. ^{1}H NMR ($CDCl_3$): δ 7.71 (s, 2H, CH_{arom}), 5.5−5.3 (br s, 1H, ArOH), 3.19 (sept, 2H, J = 6.9 Hz, CH-*i*-Pr), 2.80 (t, 2H, J = 7.4 Hz, CH_2), 1.87 (t, 2H, J = 7.4 Hz, CH_2), 1.31 (d, 12H, J = 6.9, CH_3-*i-Pr*), 1.11 (s, 3H, α-*azi*-CH_3). ^{13}C NMR ($CDCl_3$): δ 197.6 (C═O), 154.8, 133.7, 129.5, 124.3, 32.1, 28.8, 27.2, 25.7, 22.6, 20.1. HRMS (ESI) calcd for $C_{17}H_{23}N_2O_2$: [M − H] 287.1765. Found: 287.1770.

1-(4-(*tert*-Butyldimethylsilyloxy)-3,5-diisopropylphenyl)-3-(3-methyl-3*H*-diazirin-3-yl)propan-1-one (18). The diazirine **17** (100 mg, 0.347 mmol) was dissolved in the preformed mixture of *tert*-butyldimethylsilyl chloride (157 mg, 1.04 mmol), imidazole (47 mg, 0.69 mmol), and dry DMF (0.5 mL). After being stirred for 12 h at room temperature, the reaction mixture was partitioned between ether and water (10 mL each). The organic phase was washed with brine, dried over $MgSO_4$, evaporated under vacuum, and chromatographed on silica gel (2−5% of ethyl acetate in hexanes as eluent) to afford **18** as a colorless solid (120 mg, 86%), mp 48−50 °C. ^{1}H NMR ($CDCl_3$): δ 7.69 (s, 2H, H_{arom}), 3.32 (sept, 2H, J = 6.9 Hz, CH-*i*-Pr), 2.81 (t, 2H, J = 7.5 Hz, CH_2), 1.86 (t, 2H, J = 7.5 Hz, CH_2), 1.21 (d, 12H, J = 6.9, CH_3-*i*-Pr), 1.12 (s, 3H, α-*azi*-CH_3), 1.04 (s, 9H, *tert*-butyl), 0.23 (s, 6H, Si-CH_3). ^{13}C NMR ($CDCl_3$): δ 197.6 (C═O), 154.2, 139.5, 130.6, 124.0 (CH_{arom}), 32.1 (CH_2), 28.8 (CH_2), 26.7, 26.0, 25.6 (CN_2), 23.2 (CH_3-*i*-Pr), 20.1 (α-*azi*-CH_3), 18.9 (Si-CMe_3), −3.3 (Si-CH_3). HRMS (ESI) calcd for $C_{23}H_{39}N_2O_2Si$: [M + H] 403.2775. Found: 403.2377.

Solubility and Partition Properties. The solubility of **6** in 0.01 M Tris-HCL, pH 7.4, was determined by stirring excess compound in the buffer for 24 h, centrifuging at 10000*g*, and analyzing the average fraction area by reverse phase HPLC. To determine octanol/water partition coefficients of **6**, the compound was stirred in a two-phase mixture of octanol and water. Aliquots were removed from the separated phases and applied to an HPLC Proto 300 C-18 5 μm reverse-phase column (Higgins Analytical, Inc., Mountain View, CA). The UV detector was set with an absorbance wavelength of 220 nm. The mobile phase consisted of 100% acetonitrile, 0.05% TFA with a flow rate of 1 mL/min, and the average fraction area in each phase was estimated.

General Anesthetic Potency. *Xenopus laevis* tadpoles (Xenopus1, INC., Dexter, MI) in the pre-limb-bud stage (1−2 cm in length) were housed in large glass tanks filled with Amquel Plus (Kordon, Division of Novalek, Inc., Hayward, CA) treated tap water. Stock solutions of the test compound were made in ethanol. With prior approval of the MGH Subcommittee on Research Animal Care, general anesthetic potency was assessed in the tadpoles as follows. Groups of five tadpoles were placed in foil-covered 100 mL beakers containing varying dilutions of the test compound in 2.5 mM Tris HCl at pH 7.4 under low levels of ambient light. The final concentration of ethanol did not exceed 5 mM, a concentration that does not contribute to anesthesia.[32] Every 10 min tadpoles were individually flipped using the hooked end of a fire-polished glass pipet until a stable response was reached (usually at 40 min). Anesthesia was defined as the point at which the tadpoles could be placed in the supine position but failed to right themselves after 5 s (LoRR). All animals were placed in a recovery beaker of Amquel Plus treated tap water and monitored for recovery overnight. Each animal was assigned a score of either 0 (awake) or 1 (lost righting reflex), and the individual points were fit to a logistic equation by nonlinear least squares.

Electrophysiology of $GABA_A$ and *Torpedo* nACh Receptors. With prior approval by the Massachusetts General Hospital Subcommittee on Research Animal Care, oocytes were obtained from adult, female *Xenopus laevis* (Xenopus1, INC., Dexter, MI) and prepared using standard methods as previously described (see below). In vitro transcription from linearized cDNA templates and purification of subunit specific cRNAs were carried out using Ambion mMessage Machine RNA kits and spin columns. For $GABA_A$ receptor studies, oocytes were injected with ∼100 ng of total mRNA (α1, β2, γ2L) mixed at a ratio of 1:1:2 transcribed from human GABA receptor subunit cDNAs in pCDNA3.1.[33] For *Torpedo* nACh receptor studies, oocytes were injected with ∼25 ng of total mRNA mixed at a ratio of $2\alpha/1\beta/1\gamma/1\delta$ as previously described.[34]

All two-electrode voltage clamp experiments were done at room temperature, with the oocyte transmembrane potential clamped at −50 mV and with continuous oocyte perfusion with ND96 (100 mM NaCl, 2 mM KCl, 10 mM Hepes, 1 mM EGTA, 1 mM $CaCl_2$, 0.8 mM $MgCl_2$, pH 7.5) at ∼2 mL/min. Compound **6** and propofol were dissolved in DMSO at 10 mM just prior to use. Stocks were further diluted in ND96 to achieve the desired concentration.

$GABA_A$ and nACh Receptor Concentration Response and Current Inhibition Studies. All agents were applied for 15−20 s; oocytes were washed ∼3 min between each application. Currents were amplified using an oocyte clamp OC-725C amplifier (Warner Instrument Corp), digitized using a Digidata 1322A (Axon Instruments, Foster City, CA), and analyzed using Clampex/Clampfit 8.2 (Axon Instruments) and OriginPro 6.1 software. Concentration−response data were fit by nonlinear least-squares regression to the Hill (logistic) equation of the following general form:

$$I_X/I_{GABA,max} = [I_{X,max}/I_{GABA,max}] \times [1/(1 + (EC_{50}/[X])^{n_H})]$$

where [X] is the concentration of the activating ligand, $I_{GABA,max}$ is the maximally evoked current, EC_{50} is the concentration of X eliciting half of its maximal effect, and n_H is the Hill coefficient of activation. Inhibition experiments were fit with logistic equations of the following form:

$$I = 1 - ([X]^{n_H}/(IC_{50}{}^{n_H} + [X]^{n_H}))$$

Allosteric Regulation of $GABA_A$ Receptor Ligand Binding/Radioligand Binding Assays. $\alpha1\beta3\gamma2$ $GABA_A$ receptors were expressed in HEK293S-TetR cells. Homogenized cell membranes were prepared as described previously,[35] and 200 μg of $\alpha1\beta3\gamma2$ $GABA_A$ receptor membrane protein was resuspended in 500 μL of assay buffer (10 mM phosphate buffer (pH 7.4), 200 mM KCl, and 1 mM EDTA). The suspension was equilibrated with radioligands (3 nM [^{3}H]muscimol or 1.5 nM [^{3}H]flunitrazepam) and various concentrations of **6** or propofol at 4 °C for 1 h. The nonspecific binding was determined in the presence of 1 mM GABA or 1 mM flurazepam for [^{3}H]muscimol and [^{3}H]flunitrazepam binding, respectively. Next, the suspension was filtered on GF/B glass fiber filters (Whatman, Schleicher & Schuell, Maidstone, U.K.) that were pretreated in 0.5% w/v poly(ethyleneimine) for 1 h. After receptor application, filters were washed under vacuum with 7 mL of cold assay buffer and dried under a lamp for 30 min. Subsequently, they were equilibrated in Liquiscint (Atlanta, GA) and counted (Tri-Carb 1900, liquid scintillation analyzer, Perkin-Elmer/Packard, Waltham, MA).

Photoincorporation of [^{3}H]6 into the nAChR Receptor. nACh receptor-rich membranes, prepared from *Torpedo californica* electric organs as described,[36] were resuspended at 2 mg of protein/mL in *Torpedo* physiological saline (250 mM NaCl, 5 mM KCl, 3 mM $CaCl_2$, 2 mM $MgCl_2$, and 5 mM sodium phosphate, pH 7.0) supplemented with 1 mM oxidized glutathione. Aliquots (100 μL, 160 pmol of ACh binding sites) were equilibrated in glass test tubes for 30 min with 1.7 μM [^{3}H]**6** (12 Ci/mmol) in the absence or presence of other drugs. The samples were then transferred to a 96-well polyvinyl chloride microtiter plate and irradiated on ice for 30 min with a 365 nm UV lamp (Spectronics Corporation EN-16 lamp) at a distance of ∼2 cm. After irradiation, the samples were pelleted and solubilized in electrophoresis sample buffer, and equal aliquots were resolved on two 1.5 mm thick 8% acrylamide/0.33% bis-acrylamide gels. The gels were stained with Coomassie Blue R-250, and one was then treated with Amplify for fluorography and exposed to film (Biomax XAR, Kodak) for 2 weeks. For the second gel, the nAChR subunit bands were excised and quantified by liquid scintillation counting by extracting in 10% TS-2 tissue solubilizer (Research Products International Corp, Mt. Prospect, IL) and 90% ecoscint A (National

Diagnostics, Atlanta, GA) for 3 days to determine the amount of ^{3}H associated with each band.

AUTHOR INFORMATION

Corresponding Author

*Phone: (617) 726-8985. Fax: (617) 724-8644. E-mail: k_miller@helix.mgh.harvard.edu.

Author Contributions

$^{\perp}$Both of these authors contributed equally to this work.

ACKNOWLEDGMENTS

This research was supported by a grant from the National Institute for General Medicine to K.W.M. (Grant GM 58448) and by the Department of Anesthesia, Critical Care and Pain Medicine, Massachusetts General Hospital.

ABBREVIATIONS USED

ACh, acetylcholine; EC_{50}, concentration required for 50% of full effect; GABA, γ-aminobutyric acid; IC_{50}, concentration required for 50% of full inhibitory effect; LoRR, loss of righting reflexes; n_H, Hill coefficient; nACh, nicotinic acetylcholine; *p*-4-AziC5-Pro, *p*-(4-azipentyl)propofol or 2,6-diisopropyl-4-[3-(3-methyl-3*H*-diazirin-3-yl)propyl]phenol; PCP, phencyclidine; Rsn, rapsyn; TBDMS, *tert*-butyldimethylsilyl; TBPS, *tert*-butyl bicyclophosphorothionate; TFA, trifluoroacetic acid; VDAC, voltage-dependent anion channel

REFERENCES

(1) Kotani, Y.; Shimazawa, M.; Yoshimura, S.; Iwama, T.; Hara, H. The experimental and clinical pharmacology of propofol, an anesthetic agent with neuroprotective properties. *CNS Neurosci. Ther.* **2008**, *14*, 95−106.

(2) Krasowski, M. D.; Jenkins, A.; Flood, P.; Kung, A. Y.; Hopfinger, A. J.; Harrison, N. L. General anesthetic potencies of a series of propofol analogs correlate with potency for potentiation of gamma-aminobutyric acid (GABA) current at the GABA(A) receptor but not with lipid solubility. *J. Pharmacol. Exp. Ther.* **2001**, *297*, 338−351.

(3) Trapani, G.; Altomare, C.; Liso, G.; Sanna, E.; Biggio, G. Propofol in anesthesia. Mechanism of action, structure−activity relationships, and drug delivery. *Curr. Med. Chem.* **2000**, *7*, 249−271.

(4) Franks, N. P.; Lieb, W. R. Molecular and cellular mechanisms of general anaesthesia. *Nature* **1994**, *367*, 607−614.

(5) Krasowski, M. D.; Harrison, N. L. General anaesthetic actions on ligand-gated ion channels. *Cell. Mol. Life Sci.* **1999**, *55*, 1278−1303.

(6) Tanelian, D. L.; Kosek, P.; Mody, I.; MacIver, M. B. The role of the GABAA receptor/chloride channel complex in anesthesia. *Anesthesiology* **1993**, *78*, 757−776.

(7) Belelli, D.; Muntoni, A. L.; Merrywest, S. D.; Gentet, L. J.; Casula, A.; Callachan, H.; Madau, P.; Gemmell, D. K.; Hamilton, N. M.; Lambert, J. J.; Sillar, K. T.; Peters, J. A. The in vitro and in vivo enantioselectivity of etomidate implicates the $GABA_A$ receptor in general anaesthesia. *Neuropharmacology* **2003**, *45*, 57−71.

(8) Olsen, R. W.; Sieghart, W. International Union of Pharmacology. LXX. Subtypes of gamma-aminobutyric acid (A) receptors: classification on the basis of subunit composition, pharmacology, and function. Update. *Pharmacol. Rev.* **2008**, *60*, 243−260.

(9) Hanchar, H. J.; Dodson, P. D.; Olsen, R. W.; Otis, T. S.; Wallner, M. Alcohol-induced motor impairment caused by increased extrasynaptic GABA(A) receptor activity. *Nat. Neurosci.* **2005**, *8*, 339−345.

(10) Li, G. D.; Chiara, D. C.; Sawyer, G. W.; Husain, S. S.; Olsen, R. W.; Cohen, J. B. Identification of a GABAA receptor anesthetic binding site at subunit interfaces by photolabeling with an etomidate analog. *J. Neurosci.* **2006**, *26*, 11599−11605.

(11) Li, G. D.; Chiara, D. C.; Cohen, J. B.; Olsen, R. W. Numerous classes of general anesthetics inhibit etomidate binding to gamma-aminobutyric acid type A (GABAA) receptors. *J. Biol. Chem.* **2010**, *285*, 8615−8620.

(12) Nury, H.; Van Renterghem, C.; Weng, Y.; Tran, A.; Baaden, M.; Dufresne, V.; Changeux, J. P.; Sonner, J. M.; Delarue, M.; Corringer, P. J. X-ray structures of general anaesthetics bound to a pentameric ligand-gated ion channel. *Nature* **2011**, *469*, 428−431.

(13) Hall, M. A.; Xi, J.; Lor, C.; Dai, S.; Pearce, R.; Dailey, W. P.; Eckenhoff, R. G. *m*-Azipropofol (AziPm) a photoactive analogue of the intravenous general anesthetic propofol. *J. Med. Chem.* **2010**, *53*, 5667−5675.

(14) Blencowe, A.; Hayes, W. Development and application of diazirines in biological and synthetic macromolecular systems. *Soft Matter* **2005**, *1*, 178−205.

(15) Krasowski, M. D.; Hong, X.; Hopfinger, A. J.; Harrison, N. L. 4D-QSAR analysis of a set of propofol analogues: mapping binding sites for an anesthetic phenol on the GABA(A) receptor. *J. Med. Chem.* **2002**, *45*, 3210−3221.

(16) Hatanaka, Y.; Hashimoto, M.; Kurihara, H.; Nakayama, H.; Kanaoka, Y. A novel family of aromatic diazirines for photoaffinity labeling. *J. Org. Chem.* **1994**, *59*, 383−387.

(17) Hashimoto, M.; Nabeta, K.; Murakami, K. Efficient synthesis of 3-trifluoromethylphenyldiazirinyl oleic acid derivatives and their biological activity for protein kinase C. *Bioorg. Med. Chem. Lett.* **2003**, *13*, 1531−1533.

(18) Nahm, S.; Weinreb, S. M. *N*-Methoxy-*n*-methylamides as effective acylating agents. *Tetrahedron Lett.* **1981**, *22*, 3815−3818.

(19) Church, R. F. R.; Weiss, M. J. Diazirines. II. Synthesis and properties of small functionalized diazirine molecules. Observations on the reaction of a diaziridine with the iodine−iodide ion system. *J. Org. Chem.* **1970**, *35*, 2465−2471.

(20) Tonner, P. H.; Miller, K. W. Cholinergic receptors and anesthesia. *Anasthesiol., Intensivmed., Notfallmed., Schmerzther.* **1992**, *27* (2), 109−114, (Review, in German).

(21) James, R.; Glen, J. B. Synthesis, biological evaluation, and preliminary structure−activity considerations of a series of alkylphenols as intravenous anesthetic agents. *J. Med. Chem.* **1980**, *23*, 1350−1357.

(22) Trapani, G.; Latrofa, A.; Franco, M.; Altomare, C.; Sanna, E.; Usala, M.; Biggio, G.; Liso, G. Propofol analogues. Synthesis, relationships between structure and affinity at GABAA receptor in rat brain, and differential electrophysiological profile at recombinant human GABAA receptors. *J. Med. Chem.* **1998**, *41*, 1846−1854.

(23) Krasowski, M. D.; Nishikawa, K.; Nikolaeva, N.; Lin, A.; Harrison, N. L. Methionine 286 in transmembrane domain 3 of the GABAA receptor beta subunit controls a binding cavity for propofol and other alkylphenol general anesthetics. *Neuropharmacology* **2001**, *41*, 952−964.

(24) Husain, S. S.; Nirthanan, S.; Ruesch, D.; Solt, K.; Cheng, Q.; Li, G. D.; Arevalo, E.; Olsen, R. W.; Raines, D. E.; Forman, S. A.; Cohen, J. B.; Miller, K. W. Synthesis of trifluoromethylaryl diazirine and benzophenone derivatives of etomidate that are potent general anesthetics and effective photolabels for probing sites on ligand-gated ion channels. *J. Med. Chem.* **2006**, *49*, 4818−4825.

(25) Ziebell, M. R.; Nirthanan, S.; Husain, S. S.; Miller, K. W.; Cohen, J. B. Identification of binding sites in the nicotinic acetylcholine receptor for [^{3}H]azietomidate, a photoactivatable general anesthetic. *J. Biol. Chem.* **2004**, *279*, 17640−17649.

(26) Nirthanan, S.; Garcia, G. 3rd; Chiara, D. C.; Husain, S. S.; Cohen, J. B. Identification of binding sites in the nicotinic acetylcholine receptor for TDBzl-etomidate, a photoreactive positive allosteric effector. *J. Biol. Chem.* **2008**, *283*, 22051−22062.

(27) Pratt, M. B.; Husain, S. S.; Miller, K. W.; Cohen, J. B. Identification of sites of incorporation in the nicotinic acetylcholine receptor of a photoactivatible general anesthetic. *J. Biol. Chem.* **2000**, *275*, 29441−29451.

(28) Gallagher, M. J.; Cohen, J. B. Identification of amino acids of the *Torpedo* nicotinic acetylcholine receptor contributing to the binding site for the noncompetitive antagonist [(3)H]tetracaine. *Mol. Pharmacol.* **1999**, *56*, 300−307.

(29) Oswald, R. E. Effects of calcium on the binding of phencyclidine to acetylcholine receptor-rich membrane fragments from *Torpedo* californica electroplaque. *J. Neurochem.* **1983**, *41*, 1077−1084.
(30) Hamouda, A. K.; Chiara, D. C.; Blanton, M. P.; Cohen, J. B. Probing the structure of the affinity-purified and lipid-reconstituted *Torpedo* nicotinic acetylcholine receptor. *Biochemistry* **2008**, *47*, 12787−12794.
(31) Jayakar, S. S.; Dostalova, Z.; Chiara, D. C.; Zhou, X.; Liu, A.; Miller, K. W.; Cohen, J. B. Identifying an etomidate binding site in heterologously expressed human $\alpha 1\beta 3$ GABAA receptors (GABAAR) using photoactive etomidate analogs. *Biophys. J.* **2011**, *100* (3,S1), 271a.
(32) Alifimoff, J. K.; Firestone, L. L.; Miller, K. W. Anaesthetic potencies of primary alkanols: implications for the molecular dimensions of the anaesthetic site. *Br. J. Pharmacol.* **1989**, *96*, 9−16.
(33) Stewart, D.; Desai, R.; Cheng, Q.; Liu, A.; Forman, S. A. Tryptophan mutations at azi-etomidate photo-incorporation sites on alpha1 or beta2 subunits enhance GABAA receptor gating and reduce etomidate modulation. *Mol. Pharmacol.* **2008**, *74*, 1687−1695.
(34) Sullivan, D. A.; Cohen, J. B. Mapping the agonist binding site of the nicotinic acetylcholine receptor. Orientation requirements for activation by covalent agonist. *J. Biol. Chem.* **2000**, *275*, 12651−12660.
(35) Dostalova, Z.; Liu, A.; Zhou, X.; Farmer, S. L.; Krenzel, E. S.; Arevalo, E.; Desai, R.; Feinberg-Zadek, P. L.; Davies, P. A.; Yamodo, I. H.; Forman, S. A.; Miller, K. W. High-level expression and purification of Cys-loop ligand-gated ion channels in a tetracycline-inducible stable mammalian cell line: GABAA and serotonin receptors. *Protein Sci.* **2010**, *19*, 1728−1738.
(36) Middleton, R. E.; Cohen, J. B. Mapping of the acetylcholine binding site of the nicotinic acetylcholine receptor: [^{3}H]Nicotine as an agonist photoaffinity label. *Biochemistry* **1991**, *30*, 6987−6997.
(37) Tonner, P. H.; Miller, K. W. Molecular sites of general anaesthetic action on acetylcholine receptors. *Eur. J. Anaesthesiology* **1995**, *12*, 21−30, (Review).
(38) Rusch, D.; Zhong, H.; Forman, S. A. Gating allosterism at a single class of etomidate sites on alpha1beta2gamma2L GABA A receptors accounts for both direct activation and agonist modulation. *J. Biol. Chem.* **2004**, *279*, 20982−20992.
(39) Blanton, M. P.; Lala, A. K.; Cohen, J. B. Identification and characterization of membrane-associated polypeptides in *Torpedo* nicotinic acetylcholine receptor-rich membranes by hydrophobic photolabeling. *Biochim. Biophys. Acta* **2001**, *1512*, 215−224.